# DIRECT NUMERICAL SIMULATION OF PARTICLE-LADEN HOMOGENEOUS PLANE STRAIN TURBULENT FLOW

**Farzad Mashayek***
Department of Mechanical Engineering
University of Hawaii at Manoa
2540 Dole Street, Honolulu, HI 96822, USA

**Céline Barré and Dale B. Taulbee**
Department of Mechanical and Aerospace Engineering
State University of New York at Buffalo
Buffalo, NY 14260, USA

## ABSTRACT

Direct numerical simulation is utilized to generate statistics in particle-laden homogeneous plane strain turbulent flows. Assuming the two-phase flow to be dilute (one-way coupling), a variety of cases are considered to investigate the effects of the particle time constant. The carrier phase is incompressible and is treated in the Eulerian frame whereas the particles are tracked individually in a Lagrangian frame. For small particle Reynolds numbers, an analytical expression for the particle mean velocity gradient is found, which is different from the fluid one, and the dispersed phase is shown to be homogeneous. This is not the case for particles with large Reynolds numbers and no statistics involving the particle fluctuating velocity is presented for large particles. The results of the simulations are utilized to investigate the particle velocity autocorrelation, the turbulence kinetic energy, the Reynolds stresses, and the dispersion function.

## INTRODUCTION

With the increase of the interest in mathematical modeling of two-phase turbulent flows, there has been associated a growing demand for experimental and numerical studies that could lead to a more profound physical understanding of these flows in addition to a reliable data bank for model validation. During the past two decades direct numerical simulation (DNS) has emerged as an attractive means for generating accurate and detail information in turbulent flows with simple geometries. In our previous works (Taulbee *et al.*, 1997; Mashayek *et al.*, 1998), we have utilized DNS for the investigation of particle-laden isotropic and homogeneous shear turbulent flows. Our experience in implementing the DNS results for both development and assessment of turbulence models has also been very encouraging (Mashayek *et al.*, 1998). Here, we use the Fourier pseudospectral method for DNS of another mode of distortion, i.e. the irrotational plane strain flow. A very interesting feature concerning these flows is that the particle does not have the same mean velocity as its local fluid. Therefore, the DNS of these flows can be used to not only investigate the effects of the mean velocity gradients, similar to those observed in turbulent shear flows (Liljegren, 1993; Wen *et al.*, 1992; Simonin *et al.*, 1995; Taulbee *et al.*, 1997), but also to study the effects of a slip velocity between the particle and its surrounding fluid. The latter effects can be compared to the effects of gravity in isotropic turbulent flows which involve the 'crossing-trajectories effect' and the associated 'continuity effect.'

*Corresponding author: Tel: 808-956-9693, Fax: 808-956-2373, E-mail: mashaye@wiliki.eng.hawaii.edu.

## FORMULATION

This work deals with the dispersion of solid particles in a homogeneous plane strain turbulent flow. It is assumed that the two-phase flow is dilute, thus the effects of the particles on the carrier phase are neglected (i.e. one-way-coupling). The carrier phase is incompressible and is treated in the Eulerian frame and the particles are tracked in a Lagrangian manner. The continuous carrier phase is assumed to be a Newtonian fluid with constant density ($\rho_f$) and viscosity ($\mu$). With the assumption of one-way coupling, the transport of the carrier phase is not influenced by the presence of the particles, and is described via the Eulerian continuity and momentum equations:

$$\frac{\partial \widehat{U}_j}{\partial x_j} = 0, \quad \frac{\partial \widehat{U}_i}{\partial t} + \frac{\partial}{\partial x_j}(\widehat{U}_i \widehat{U}_j) = -\frac{\partial \widehat{P}}{\partial x_i} + \frac{1}{Re_0}\frac{\partial^2 \widehat{U}_i}{\partial x_j \partial x_j} \quad (1)$$

where $\widehat{\ }$ denotes the instantaneous variable, $x_i$ and $t$ are the spatial and temporal coordinates, respectively, and $\widehat{U}_i$ and $\widehat{P}$

indicate the fluid instantaneous velocity and pressure, respectively. All the variables are normalized by the reference length ($L_0$), density ($\rho_0$), and velocity ($U_0$) scales. The length scale is conveniently chosen such that the normalized volume of the simulation box is $(2\pi)^3$, and the fluid density is used as the scale for density. The velocity scale is found from the specified box Reynolds number, $Re_0 = \rho_0 U_0 L_0/\mu$.

To configure the plane strain flow, the carrier phase is subjected to a uniform mean strain in two directions such that: $\widehat{U}_i = Sx_1\delta_{i1} - Sx_2\delta_{i2} + u_i$, where $\delta_{ij}$ is the Kronecker delta function and $u_i$ is the carrier phase fluctuating velocity. The magnitude of the imposed strain is given by $S = \partial U_1/\partial x_1 = -\partial U_2/\partial x_2 = \text{const.}$, where $U_i =< \widehat{U}_i >$ denotes the Eulerian ensemble-mean (denoted by $< >$) velocity. The geometry is defined by the Cartesian coordinates $x_1$ (stretched direction), $x_2$ (squeezed direction), and $x_3$ (invariant direction). With this mean velocity gradient, Lee and Reynolds (1985) show that the turbulence is homogeneous. Such a flow is, in concept, unbounded, however, in numerical simulations a finite domain may be considered by applying periodic boundary conditions which allows utilization of the Fourier spectral method. This is accomplished by solving the governing equations for fluctuating velocities on a grid which deforms with the mean flow. This transformation has been discussed in detail by Rogallo and Moin (1984) and is only summarized here. A computational (deforming) coordinate system, $x_i'$, is related to the fixed (non-deforming) system through $x_i' = B_{ij}(t)x_j$ where the transformation tensor is defined as:

$$B_{ij}(t) = \begin{pmatrix} B_{11}^0 \exp(-St) & 0 & 0 \\ 0 & B_{22}^0 \exp(St) & 0 \\ 0 & 0 & B_{33}^0 \end{pmatrix} \qquad (2)$$

where superscript '0' refers to the value of $B_{ij}$ at $t = 0$. Applying the transformation, the governing equations for the carrier phase in the deforming coordinate system are expressed as:

$$B_{ji}\frac{\partial u_i}{\partial x_j'} = 0,$$

$$\frac{\partial u_i}{\partial t'} + U_{i,j}u_j + B_{mj}\frac{\partial (u_i u_j)}{\partial x_m'} + B_{mi}\frac{\partial p}{\partial x_m'} = \frac{B_{mj}B_{nj}}{Re_0}\frac{\partial^2 u_i}{\partial x_m' \partial x_n'} \qquad (3)$$

The solid particles are assumed to be spherical with diameter smaller than the smallest length scale of the turbulence. Since the volume fraction of the dispersed phase is small, the particle-particle collisions can be neglected. The particle density is much larger than the fluid density such that only the drag force and inertia are significant to the particle dynamics. Therefore, the Lagrangian equations of motion for the discrete particles reduce to:

$$\frac{d\widehat{X}_i}{dt} = \widehat{V}_i, \quad \frac{d\widehat{V}_i}{dt} = \frac{f}{\tau_p}\left(\widehat{U}_i^* - \widehat{V}_i\right) \qquad (4)$$

where $\widehat{X}_i$ and $\widehat{V}_i$ are the particle instantaneous position and velocity, respectively. The superscript * indicates the fluid variable evaluated at the particle location. The particle time constant for Stokesian drag of a spherical particle is defined as $\tau_p = Re_0 \rho_p d_p^2/18$ where $\rho_p$ and $d_p$ are the nondimensional particle density and diameter, respectively. The particle variables are normalized using the same reference scales as those used for the carrier phase variables. The parameter $f = 1 + 0.15Re_p^{0.687}$ describes an empirical correction to Stokesian drag for large particle Reynolds numbers ($Re_p = Re_0 d_p|\widehat{U}_i^* - \widehat{V}_i|$) and is valid for $Re_p < 1000$ (Wallis, 1969).

We have seen that the carrier phase is homogeneous and that provided a linear transformation, periodic boundary conditions can be applied to the turbulent plane strain flow. The extension of this transformation to the dispersed phase, however, is not straightforward as the particles do not have the same mean velocity as that of the carrier phase. To make this point clear, we consider the average particle momentum equation:

$$\frac{D^V V_i}{Dt} = \ll \frac{f}{\tau_p}(\widehat{U}_i^* - \widehat{V}_i) \gg - \ll v_j \frac{\partial v_i}{\partial x_j} \gg \qquad (5)$$

where $\frac{D^V}{Dt} = \frac{\partial}{\partial t} + V_j \frac{\partial}{\partial x_j}$, the notation $\ll \gg$ denotes the ensemble average associated with the dispersed phase, and $V_i$ ($= \ll \widehat{V}_i \gg$) and $v_i$ are the particle mean and fluctuating velocity, respectively. It is noted that, if $U_i^*$ stands for the Eulerian mean fluid velocity at the particle position, $V_i = U_i^*$ is not a solution to (5) except for $\tau_p \to 0$. As a result, there always exists a relative mean velocity between the two phases which can result in large particle Reynolds numbers, especially far from the origin.

For small particle Reynolds numbers, letting $f = 1$ in the averaged particle momentum equation (5) leads to:

$$\frac{D^V V_i}{Dt} = \frac{1}{\tau_p}\left(\ll \widehat{U}_i^* \gg - V_i\right) - \ll v_j \frac{\partial v_i}{\partial x_j} \gg \qquad (6)$$

Provided that the initial particle velocity fluctuation is isotropic and the initial particle mean velocity is such that $V_\alpha(0) = \sigma_\alpha^0 x_\alpha(0)$ where $\sigma_\alpha^0$ is a constant ($\alpha = 1,2,3$ with no summation on Greek indices), Barré (1998) shows that the following propositions are equivalent: (i) The dispersed phase remains homogeneous. (ii) The correlation $\ll v_j \frac{\partial v_i}{\partial x_j} \gg$ is identically zero. (iii) $\exists \sigma_\alpha \; \forall t \; V_\alpha(x_j,t) = \sigma_\alpha(t)x_\alpha$. The proof of the above statements is very lengthy; we refer to Barré (1998) and here only present the final results for the mean velocity of the dispersed phase in tables 1-3.

The knowledge of the particle mean velocity allows the calculation of the statistics involving the particle fluctuating velocity for cases with small particle time constant. The analytical solution for the mean velocity of small particles also shows the existence of a critical particle time constant (denoted by $\tau_{p_{cr}}$ in tables 1-3) beyond which the particles follow an oscillatory trajectory about the elongated ($x_1$) axis. For large particles, the empirical correction added to the drag coefficient prevents a homogeneous solution for the dispersed phase. The results generated for large particles are mainly used to study the dispersion characteristics of the particles.

Table 1: Particle mean velocity in $x_1$-direction.

| $V_1(t) = \sigma_1(t)x_1,\ \sigma_1(0) = \sigma_1^0$ | | |
|---|---|---|
| condition on $\tau_p$ | initial condition | solution for $V_{1,1}(t)$ |
| any $\tau_p$ | $\sigma_1^0 \neq \xi_1$ | $\sigma_1(t) = \dfrac{\eta_1 \exp(\eta_1 t) + \dfrac{\sigma_1^0 - \eta_1}{\xi_1 - \sigma_1^0}\xi_1 \exp(\xi_1 t)}{\exp(\eta_1 t) + \dfrac{\sigma_1^0 - \eta_1}{\xi_1 - \sigma_1^0}\exp(\xi_1 t)}$<br>$\xi_1 = \dfrac{-1+\sqrt{1+4S\tau_p}}{2\tau_p}$<br>$\eta_1 = \dfrac{-1-\sqrt{1+4S\tau_p}}{2\tau_p}$ |
| | $\sigma_1^0 = \xi_1$ | $\sigma_1(t) = \xi_1 = \text{constant}$ |

Table 2: Particle mean velocity in $x_2$-direction.

| $V_2(t) = \sigma_2(t)x_2,\ \sigma_2(0) = \sigma_2^0$ | | |
|---|---|---|
| condition on $\tau_p$ | initial condition | solution for $V_{2,2}(t)$ |
| $\tau_p < \tau_{p_{cr}}$<br>$\left(\tau_{p_{cr}} = \frac{1}{4S}\right)$ | $\sigma_2^0 \neq \xi_2$ | $\sigma_2(t) = \dfrac{\eta_2 \exp(\eta_2 t) + \dfrac{\sigma_2^0 - \eta_2}{\xi_2 - \sigma_2^0}\xi_2 \exp(\xi_2 t)}{\exp(\eta_2 t) + \dfrac{\sigma_2^0 - \eta_2}{\xi_2 - \sigma_2^0}\exp(\xi_2 t)}$<br>$\xi_2 = \dfrac{-1+\sqrt{1-4S\tau_p}}{2\tau_p}$<br>$\eta_2 = \dfrac{-1-\sqrt{1-4S\tau_p}}{2\tau_p}$ |
| | $\sigma_2^0 = \xi_2$ | $\sigma_2(t) = \xi_2 = \text{constant}$ |
| $\tau_p = \tau_{p_{cr}}$ | $\sigma_2^0 \neq -\frac{1}{2\tau_p}$ | $\sigma_2(t) = \dfrac{\sigma_2^0 - \left(\sigma_2^0 + \dfrac{1}{2\tau_p}\right)\dfrac{t}{2\tau_p}}{1 + \left(\sigma_2^0 + \dfrac{1}{2\tau_p}\right)t}$ |
| | $\sigma_2^0 = -\frac{1}{2\tau_p}$ | $\sigma_2(t) = -\frac{1}{2\tau_p} = \text{constant}$ |
| $\tau_p > \tau_{p_{cr}}$ | any $\sigma_2^0$ | $\sigma_2(t) = \dfrac{\sigma_2^0 + \dfrac{-1}{2\tau_p\omega}(\sigma_2^0 + 2S)\tan(\omega t)}{1 + \dfrac{\sigma_2^0 + \frac{1}{2\tau_p}}{\omega}\tan(\omega t)}$<br>$\omega = \dfrac{\sqrt{4S\tau_p - 1}}{2\tau_p}$ |

Table 3: Particle mean velocity in $x_3$-direction.

| $V_3(t) = \sigma_3(t)x_3,\ \sigma_3(0) = \sigma_3^0$ | | |
|---|---|---|
| condition on $\tau_p$ | initial condition | solution for $V_{3,3}(t)$ |
| any $\tau_p$ | $\sigma_3^0 \neq 0$ | $\sigma_3(t) = \dfrac{\exp\left(\dfrac{-t}{\tau_p}\right)}{\dfrac{1+\tau_p\sigma_3^0}{\sigma_3^0} - \tau_p \exp\left(\dfrac{-t}{\tau_p}\right)}$ |
| | $\sigma_3^0 = 0$ | $\sigma_3(t) = 0$ |

## RESULTS

A Fourier pseudospectral method with triply periodic boundary conditions is employed for the spatial representation of the fluid velocity and pressure. Temporal advancement of the Lagrangian particle equations is done by the second-order accurate Adams-Bashford method. In order to evaluate fluid variables at the particle locations a fourth order accurate Lagrange polynomial interpolation scheme is employed. The initial conditions for the plane strain runs are obtained by preliminary simulations of homogeneous decaying turbulence (Lee and Reynolds, 1985). During the plane strain runs, the computational domain becomes elongated (shortened) in the direction of positive (negative) mean strain rates. To allow the simulations continue for a longer time, we implement a predistorted initial mesh with short side in the direction to be elongated by positive mean strain rate and vice versa. For the carrier phase, the initial aspect ratio for the computational domain is $1/2:2:1$ ($B^0_{11}=2$, $B^0_{22}=1/2$, $B^0_{33}=1$), and at the final simulation time this becomes $2:1/2:1$ ($B_{11}=1/2$, $B_{22}=2$, $B_{33}=1$). If we define the reference total strain as $c=\exp(St)$, each strain run is performed until the reference total strain reaches approximately 4.

For a given mean strain rate ($S=0.739$), we have considered eight cases to investigate the effects of the particle time constant, using $1.2\times10^5$ particles on $96^3$ grid points. For all the simulations $\rho_p=721.8$ is used. The mean velocity gradient of the dispersed phase is initially imposed as:

$$V_{i,j}(0)=\begin{pmatrix}\xi_1 & 0 & 0\\ 0 & -S & 0\\ 0 & 0 & 0\end{pmatrix} \qquad (7)$$

In this manner, for homogeneous dispersed phase $V_{i,j}(t)=V_{i,j}(0)$ =const. for any $t$, if $i\neq 2$ and $j\neq 2$. Also, $V_{2,2}(t,\tau_{p1})\leq V_{2,2}(t,\tau_{p2})$ if $\tau_{p1}<\tau_{p2}$ for the range of time considered in the present simulations. To demonstrate the accuracy of the single phase flow simulation, the present DNS results were compared to those from the DNS of Rogallo and Moin (1984) and Lee and Reynolds (1985), and the experiment of Tucker and Reynolds (1968).

First, we discuss the results for cases in which the dispersed phase can be considered homogeneous. For these cases, the Lagrangian autocorrelation coefficient of the particle velocity is defined as:

$$R_{\alpha\alpha}(t)=\frac{\ll v_\alpha(t_0)v_\alpha(t_0+t)\gg}{\ll v^2_\alpha(t_0)\gg^{\frac{1}{2}}\ll v^2_\alpha(t_0+t)\gg^{\frac{1}{2}}} \qquad \alpha=1,2,3 \quad (8)$$

where $t_0$ is the time at which we start computing the Lagrangian statistics. Since the turbulence is non-stationary, the value of $R_{\alpha\alpha}$ depends on the choice of $t_0$. The total time in our plane strain simulations is somewhat short, therefore, we choose to take $t_0=0$ which is the starting time for plain strain simulations. The autocorrelation coefficient for various $\tau_p$ values are shown in Fig. 1 along with that of the massless fluid particle. It is observed that, for short dispersion times, the 'memory' of the particle to its previous velocity is increased as the particle inertia increases, thus increasing the autocorrelation coefficient. For $\tau_p>\tau_{p_{cr}}(=0.338)$ the magnitude of the particle autocorrelation exceeds that of the fluid particle. At later times, the autocorrelation of these heavier particles cross over that of the fluid such that at long times the particle velocities are less correlated than the fluid velocities. This is again due to the particle inertia. At long times, the solid particle continues to interact with new fluid elements and thus $R_{\alpha\alpha}$ decays at a faster rate than that of the fluid. In all three directions, a crossing is observed for the autocorrelation curves of various $\tau_p$. The crossing occurs sooner in the $x_2$-direction and for the autocorrelation curves of $\tau_p=0.112$ and $\tau_p=0.225$. This suggests that particles with high inertia change their surrounding fluid more rapidly and tend to lose correlation with their previous velocity faster than a lighter particle does. In plane strain flows, the particle mean velocity depends on the particle time constant and in our simulations the relative mean velocity between the particle and its surrounding fluid increases with the increase of $\tau_p$. Thus particles with higher inertia are more subjected to 'crossing-trajectories' effects than lighter ones, and the decay rate of $R_{\alpha\alpha}$ increases with $\tau_p$ at long times causing the autocorrelation to become smaller for larger particle time constant. Figure 1 also shows that the autocorrelation of the particle velocity in the shortened direction ($x_2$) is larger than that in both elongated ($x_1$) and spanwise ($x_3$) directions.

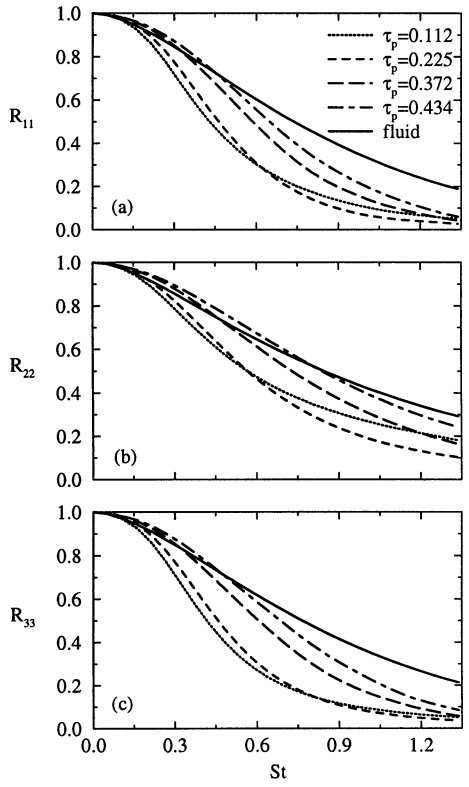


Figure 1: Effect of $\tau_p$ on the particle velocity autocorrelation and comparison with the fluid velocity autocorrelation.

The effects of the particle inertia on the evolution of the particle turbulence kinetic energy appear in Fig. 2. All the

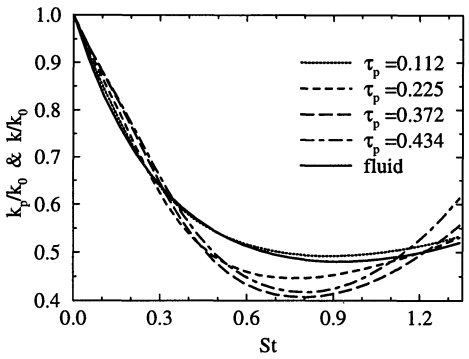


Figure 2: Temporal variations of the turbulence kinetic energy for the fluid ($k$) and the particles ($k_p$) for different values of the particle time constant.

kinetic energies shown in this figure are normalized by $k_0$, the turbulence kinetic energy of the fluid at the initial time. It is observed that during the early dispersion times, the normalized particle turbulence kinetic energy is larger than the fluid one, and increases with the increase of particle inertia. Later, the fluid turbulence kinetic energy starts to level off and $k_p$ continues to decay at a faster rate than $k$. Because the decay rate of $k_p$ is larger for smaller inertia particles, the time at which the particle turbulence kinetic energy decreases below that of the fluid is shorter for smaller particles. At long dispersion times, the particle turbulence kinetic energy increases over that of the fluid for all cases. Increasing the particle time constant results in a larger growth rate for the particle turbulence kinetic energy for long times.

The temporal variation of the normal Reynolds stresses of the fluid ($< u_\alpha^2 >$) and particles ($\ll v_\alpha^2 \gg$), and the fluid-particle velocity covariance ($\ll u_\alpha^* v_\alpha \gg$) are shown in Fig. 3. The particle Reynolds stress in $x_2$-direction ($\ll v_2^2 \gg$) is strongly affected by the mean velocity gradient. It is considerably larger than the corresponding fluid-particle velocity covariance ($\ll u_2^* v_2 \gg$), and exceeds the fluid Reynolds stress ($< u_2^2 >$). These features are even more pronounced when the particle time constant increases. It is also observed that an increase of particle inertia decreases the fluid-particle velocity covariance, below the value of $< u_2^2 >$, due mainly to strong decorrelation of the fluid and particle velocity at larger $\tau_p$. These results are in general agreement with theoretical results of Reeks (1993) and Liljegren (1993) regarding the effect of a mean fluid velocity gradient on the streamwise particle velocity variance in shear flows. However, the non-zero mean fluid velocity gradient component in the stretched direction ($U_{1,1} = S$) does not affect $\ll v_1^2 \gg$ similarly to that in the squeezed ($x_2$) direction. In the analysis of Liljegren (1993) the term responsible for the increase of the streamwise particle velocity variance above the fluid one is proportional to $-V_{1,2} \ll v_1 v_2 \gg$ which is positive in the case of shear flow. Here, the fluid mean velocity gradient results in a positive particle mean velocity gradient component $V_{1,1}$. Thus, the term $-V_{1,1} \ll v_1^2 \gg$ in the transport equation of $\ll v_1^2 \gg$ behaves like a dissipation and decreases the particle Reynolds stress

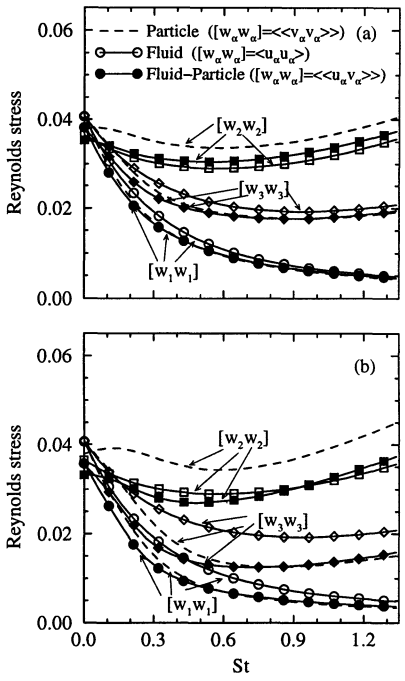


Figure 3: Temporal evolution of the Reynolds stress components of the fluid and the particles and the fluid-particle covariance. Hollow and filled symbols refer to the fluid and the fluid-particle, respectively. (a) $\tau_p = 0.112$, (b) $\tau_p = 0.225$.

in $x_1$-direction below that in $x_3$-direction. Moreover, $V_{1,1}$ is larger than $U_{1,1}$ and increases with particle inertia. This could explain that the particle velocity variance in the elongated direction is smaller than the fluid one and decreases with increasing $\tau_p$ (although a direct analogy with Liljegren (1993) theory is not attempted here). In the spanwise direction, the particle velocity variance is not directly affected by the mean velocity gradients and consistent with the results for shear flow in the normal or spanwise directions, it remains below the corresponding fluid turbulent stresses and, given sufficient development time, becomes nearly equal to the fluid-particle velocity covariance. An inspection of Fig. 3 shows that the particle velocity variance in the spanwise direction decreases when the particle time constant increases.

In order to quantify the dispersion of the particles, the dispersion function (or r.m.s. displacement) of a solid or fluid particle in the $x_\alpha$-direction is calculated from:

$$D_{\alpha\alpha}(t) = \left[ \frac{1}{N} \sum_{i=1}^{N} \left( \widehat{X}_\alpha^{(i)}(t) - X_\alpha^{inj} \right)^2 \right]^{\frac{1}{2}} \qquad (9)$$

where $N$ is the total number of particles in the flow field at time $t$, $\widehat{X}_\alpha^{(i)}$ is the instantaneous position of particle $(i)$ at time $t$, and $X_\alpha^{inj}$ is the injection location of the same particle. Here, we consider both the homogeneous and the inhomogeneous dispersed phases. Figure 4 shows the variation of the dispersion function with time for various particle time constants

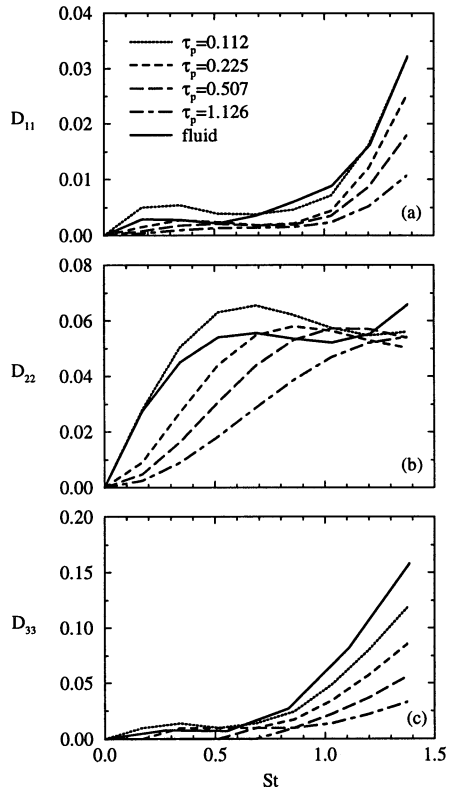


Figure 4: Dispersion function for fluid and solid particles for different particle time constants; particles injected at $X_1^{inj} = 0.01$, $X_2^{inj} = 0.01$, and $X_3^{inj} = \pi$.

for an injection location close to the $x_3$-axis ($X_1^{inj} = 0.01$, $X_2^{inj} = 0.01$, $X_3^{inj} = \pi$). The dispersion function generally increases with time since the particles disperse increasingly farther from their injection location. At earlier times, the dispersion seems to be the highest for $\tau_p = 0.112$, whereas at longer times the fluid particles exhibit the highest amount of dispersion. It is observed that for long times the dispersion in $x_1$ and $x_3$ directions decreases significantly as the inertia increases. The reason is that, as the turbulence fluctuations grow in time, it becomes more difficult for larger particles to follow the turbulent motions. This is similar to the results calculated by Yeh and Lei (1991) in the case of homogeneous turbulent shear flows.

## CONCLUSION

Results obtained by direct numerical simulation (DNS) have been used to investigate particle-laden homogeneous plane strain turbulent flows. An analysis of the averaged equations of motion for the dispersed phase indicates that there is always a relative mean velocity between the particle and its surrounding fluid. Under the assumption of small particle Reynolds number, the dispersed phase is shown to be homogeneous and an analytical solution is found for the particle mean velocity. This allows the calculation of the statistics involving the particle fluctuating velocity for cases with small particle time constant. The analytical solution for the mean velocity of small particles also shows the existence of a critical particle time constant beyond which the particles follow an oscillatory trajectory about the elongated ($x_1$) axis. For large particles, the empirical correction added to the drag coefficient prevents a homogeneous solution for the dispersed phase. The results generated for large particles are mainly used to study the dispersion characteristics of the particles.

## REFERENCES


Barré, C. (1998), Direct numerical simulation of particle-laden plane strain turbulent flows. M.S. Thesis, Department of Mechanical and Aerospace Engineering, State University of New York at Buffalo, Buffalo, NY.

Lee, M. J. and Reynolds, W. C. (1985). Numerical experiments on the structure of homogeneous turbulence. Department of Mechanical Engineering Report TF-24, Stanford University, Stanford, CA.

Liljegren, L. M. (1993). The effect of a mean fluid velocity gradient on the streamwise velocity variance of a particle suspended in a turbulent flow. *Int. J. Multiphase Flow* **19**, 471–484.

Mashayek, F., Taulbee, D. B., and Givi, P. (1998). Modeling and simulation of two-phase turbulent flow. In Roy, G. D., editor, *Propulsion Combustion: Fuels to Emissions*, chapter 8, pages 241–280. Taylor & Francis, Washington, D.C.

Reeks, W.M. (1993). On the constitutive relations for dispersed particles in nonuniform flows. I: Dispersion in a simple shear flow. *Phys. Fluids* **5**, 750–761.

Rogallo, R. S. and Moin, P. (1984). Numerical simulation of turbulent flow. *Ann. Rev. Fluid Mech.* **16**, 99–137.

Simonin, O., Deutsch, E., and Boivin, M. (1995). Large eddy simulation and second-moment closure model of particle fluctuating motion in two-phase turbulent shear flows. In Durst, F., Kasagi, N., Launder, B.E., Schmidt, F.W., and Whitelaw, J.H., editors, *Turbulent Shear Flows 9*, pages 85–115. Springer-Verlag.

Taulbee, D. B., Mashayek, F., Givi, P., and Barré, C. (1997). Simulation and Reynolds stress modeling of particle-laden turbulent shear flows. In *the Proceedings of the 11th Symp. on Turbulent Shear Flows*, Grenoble, France.

Tucker, H. J. and Reynolds, A. J. (1968). The distortion of turbulence by irrotational plane strain. *J. Fluid Mech* **32**, 657–673.

Wallis, G. B. (1969). *One Dimensional Two Phase Flow*. McGraw Hill, New York, NY.

Wen, F., Kamalu, N., Chung, J. N., Crowe, C. T., and R., Troutt T. (1992). Particle dispersion by vortex structures in plane mixing layers. *J. Fluids Eng.* **114**, 657–666.

Yeh, F. and Lei, U. (1991). On the motion of small particles in a homogeneous turbulent shear flow. *Phys. Fluids* **3**, 2758–2776.